An Actuator-Disc Model for the Prediction of Abrupt Stall in an Axial Compressor Rotor

A. J. Al-Daini* and J. W. Railly†

The representation of loss in a cascade by the appearance of blockage has been extended to deal with blade rows by the use of a source distribution to represent this blockage, and in the case of the actuator disc approximation, the presence of sources is confined to an axi-symmetric distribution over the actuator disc. It is found that if a typical dependence of loss (and consequently diffusion ratio) upon incidence for each section of an axial compressor rotor is represented in this manner, the influence of blockage on the axial velocity distribution may be found using the potential equation combined with the usual actuator disc approximation. Study of the behaviour of the controlling ordinary differential equation for the axial velocity ahead of the disc reveals that as the flow is reduced, the equation contains a singularity within the range of radius and a meaningful solution does not exist. This result is interpreted as the limit to continuous operation and reasonable agreement between this predicted limit and the appearance of abrupt stall (experimentally) is found.

NOTATION

A_2, A_3	the restricted and the total area between blades (Figure 1)
A, B	as defined in eq. (16)
$C(r)$	this is defined in Appendix 1
D	diffusion ratio defined by $V_{2,id}/V_1$
D'	$dD/d \cot \beta_1$
D'_s	the value of D' at which abrupt stall commences
D_m	the minimum diffusion factor
$E(r)$	as defined in Appendix 1
$f(r)$, $F(r)$	functions of r, eqs (7) and (9)
h	blade height
$H^{(R)}$	total head relative to rotor
$H(+\infty)$, $H(-\infty)$	the total head at $+\infty$ and $-\infty$, respectively
k	π/h
P	static pressure
r	radius
S	source strength
S_r	dS/dr
t_2	$\tan \beta_2$
t'_2	$d \tan \beta_2/dr$
$V_{2,id}$	the total velocity of the flow at blade outlet
V_1	the total inlet velocity of the flow at blade inlet
V_z, V_r, V_θ	axial, radial, and tangential components of velocity
V'_z, V''_z	axial velocity at blade inlet and outlet, respectively
$V_{z,-\infty}$, $V_{z,+\infty}$	axial velocity at $-\infty$ and $+\infty$, respectively
$V_{z,0}$	axial velocity exactly in the plane source/actuator disc
V_{r-}, V_{r+}	radial velocity at blade inlet and blade outlet, respectively
V''_θ	tangential component of velocity at blade outlet
X_s	loss coefficient defined by $(H_1^{(R)} - H_2^{(R)})/(\frac{1}{2}V_1^2)$
Y	$\cos \beta_1/\cos \beta_2$
Z	axial direction
α	the blockage ratio equal to A_2/A_3 (Fig. 1)
α_m	the blockage ratio at minimum diffusion ratio
β_1, β_2	relative inlet and outlet angles for source/actuator disc
ζ	density
ϕ_s	the potential of the source flow
$\phi_{t,n}$	overall flow coefficient at which neutral stability is satisfied
$\phi_{t,c}$	the singularity limit overall flow coefficient
ψ_2	total to static pressure coefficient defined by $(P''_2/\rho - H_1)/(\frac{1}{2}\Omega^2 r^2)$
ψ_{2t}	overall total to static pressure coefficient based on tip speed
Ω	rotor speed in rad/sec

INTRODUCTION

Examination of the stability of isolated aerofoil compressor cascades, for example, Stenning and Kriebel (1), reveal that non-uniform flow (in the form of waves travelling along the cascade axis) will develop if the slope of the loss-incidence curve is sufficiently high. In the work above quoted, instead of loss, a blockage ratio, α, is introduced (see Fig. 1) which is related to the loss coefficient, X_s, as follows:

$$\frac{1}{\alpha^2} = 1 + X_s \frac{\cos^2 \beta_2}{\cos^2 \beta_1} \tag{1}$$

The theory then shows that the above instability occurs when

$$\frac{d\alpha}{d(\cot \beta_1)} = \frac{\alpha}{\cot \beta_1} \tag{2}$$

* Research Student, Department of Mechanical Engineering, University of Birmingham.
† Professor of Turbomachinery, Department of Mechanical Engineering, University of Birmingham.
Received on 15 May 1979 and accepted for publication on 16 July 1979.

0142/727X/79/0900-0099$02.00

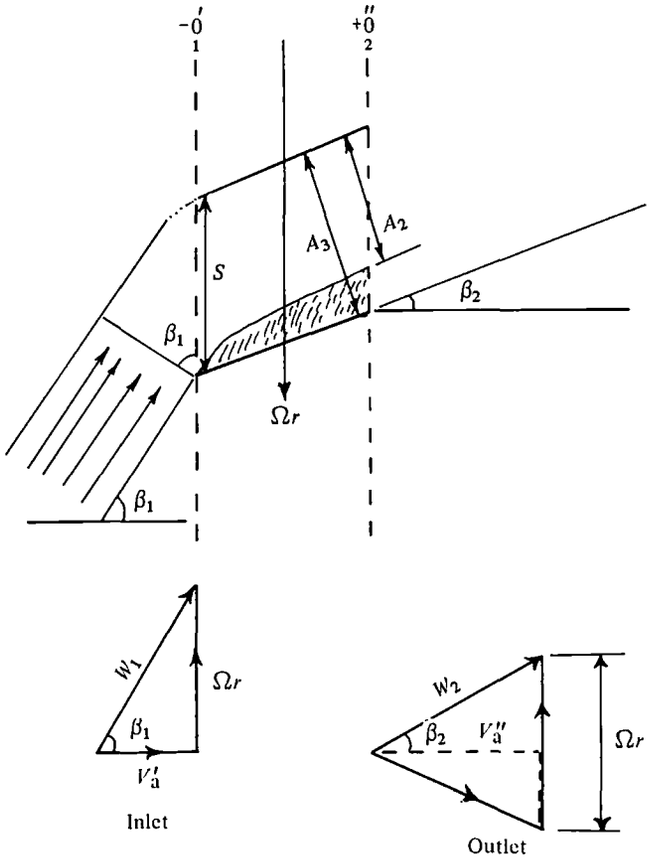

Fig. 1. Flow model

In the case of an isolated rotor row (of hub/tip ratio close to unity) eq. (2) is the same as

$$\frac{d\psi_2}{d(\cot \beta_1)} = 0 \tag{3}$$

where ψ_2 is the total-to-static pressure rise coefficient.

When the performance of an actual rotor row is considered, it would seem reasonable to test the performance, at each radius, in terms of eq. (3). It is frequently found that the point of abrupt stall coincides with the presence of the above condition at some radius. It is also found that there are appreciable regions where the condition is complied with but abrupt stall fails to appear; the experimental pressure-volume characteristic depicted in Fig. 7 demonstrates such a behaviour; data on this rotor is given in Appendix 2. Furthermore, it is evident that abrupt stall occurs sharply, with accurate repeatability (in terms of throttle setting) and quite without warning. In the search for more effective criteria for stall prediction an alternative steady flow performance model was formulated. The model chosen for investigation was one which incorporated a loss model which, it was thought, would represent the more important aspects of loss on the flow distribution. In practice, losses arise as a consequence (for some reason or another) of flow separation within the blading. The actual loss mechanism, namely, the 'mixing-out' of the eddies produced by this separation, is highly complex but tends to occur downstream of the trailing edges and thus might not have much effect ahead of the row. On the other hand, the separation process behaves as if the flow passing through the blades were 'blocked'; in fact, this mechanism is that used by Stenning and Kriebel in their study of stability. In a rotor, the blockage which occurs at any particular radius will correspond to the local incidence condition and, therefore, must vary more strongly over the radius as the flow coefficient is reduced.

In the following treatment, the potential flow effects of this varying blockage will be represented by a source distribution in the plane of the rotor row. In fact, since the rotor row may be replaced by an actuator disc, the blockage influence may be represented by a source-disc co-incidental with the former. The source intensity S (at any radius) will be defined using the same flow description as in the definition of α above, and the actual value of the former must rest upon some suitable hypothesis in regard to its dependence on incidence. The representation of the blade row performances in these terms is discussed below, and the resulting axi-symmetric flow which occurs as a consequence of the superposition of a source-disc on to an actuator disc is explored.

REPRESENTATION OF LOSS BY A SOURCE DISTRIBUTION

Referring to Fig. 1, it is evident that the area, A_3, at the blade row exit is reduced as a consequence of the separation, which results in the appearance of a stagnant zone. From the viewpoint of the flow ahead of the row, this stagnant zone may be satisfactorily represented by a source output just adequate to fill the stagnant zone with fluid having the same velocity as the existing 'jet', namely, $V_{2,id}$ which may be assumed to be flowing at the angle of the normally attached flow, namely, β_2. The axial component of velocity behind the row, V''_z, in the presence of sources, must thus be larger than that entering. In fact, the source intensity per unit area of disc must be given (see Fig. 2) by:

$$S = V''_z - V'_z \tag{4}$$

In terms of the blockage ratio, α, it follows also that:

$$\alpha = A_2/A_3 = \frac{V_2}{V_{2,id}} = \frac{V'_z}{V''_z} \tag{5}$$

Introducing the diffusion ratio, D, given by

$$D = \frac{V_{2,id}}{V_1} \tag{6}$$

it may be seen that the pressure change across the row may be calculated by applying Bernouilli's equation in the absence of loss between '1' and '2'. In practice, momentum mixing (in the absence of sources) will occur downstream giving a pressure rise and an increase in outlet angle. It is an assumption of this work that this mixing occurs sufficiently far away from the trailing

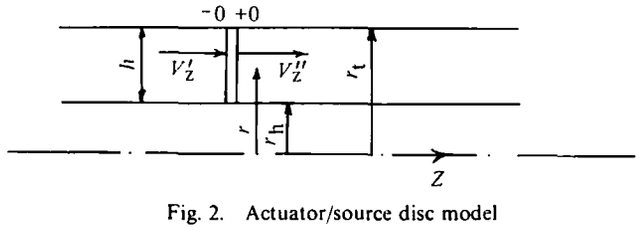

Fig. 2. Actuator/source disc model

edges to allow the ignoring of its influence upon the three-dimensional (axi-symmetric) flow. In that event, the source output may be assumed to be present in the flow field to downstream infinity of the disc.

MODIFIED ACTUATOR DISC SOLUTION

In actuator disc theory, for example, Marble (**2**), it is demonstrated that the radial velocity may be found from the solution of a linear equation and it is frequently assumed that a single term approximation is adequate, namely,

$$V_r = f(r)\, e^{\pm kz} \tag{7}$$

which is appropriate to an isolated rotor in a long cylindrical annulus.

In this expression it has been assumed that the radial velocity is continuous across the disc in common with the usual requirement of radial blades. It should be noted that the above solution for the source disc also leads to continuity of the radial component of velocity, but at the same time there is a change in the radial momentum flux across the disc (associated with the change in the axial component of velocity), even with zero stagger blading.

In the formulation of the boundary conditions to be satisfied, the above velocity is usually neglected in comparison with the whirl and axial components when these latter are combined in the equation of motion. Consequently, since the presence of a source disc will give rise to a further field of radial velocity, it is permissible to add these fields together in the process of finding the resulting distribution of axial velocities. Considering the source disc, therefore, in isolation, the resulting flow may be seen to arise from the solution of the potential equation in cylindrical polar co-ordinates, with the boundary conditions on either side of the disc given by

$$S = \left(\frac{\partial \phi_s}{\partial z}\right)_{z=+0} - \left(\frac{\partial \phi_s}{\partial z}\right)_{z=-0} \tag{8}$$

where ϕ_s is the potential of the source flow of which the first term solution may be given by:

$$\phi_s = F(r)\, e^{\pm kz} \tag{9}$$

and the total potential is $V_{z_0} z + \phi_s$. Then $F(r)$ may be written in terms of S and, further,

$$\left.\begin{aligned} V_{r_-} &= -\left(\frac{S_r}{2k}\right) e^{kz}, \qquad z<0 \\ V_{r_+} &= -\left(\frac{S_r}{2k}\right) e^{-kz}, \qquad z>0 \end{aligned}\right\} \tag{10}$$

are the radial velocity components due to this source distribution; the suffix on S implies differentiation with respect to radius. In eqs (7) and (9), it will be sufficiently accurate to take k from the solution of the Laplace equation in rectangular co-ordinates (corresponding to a hub/tip ratio close to unity), which, being in terms of trigonometric functions, gives the usual value π/h for both constants.

From the equation of continuity in cylindrical polar form (in axial symmetry)

$$\frac{1}{r}\frac{\partial}{\partial r}(rV_r) + \frac{\partial V_z}{\partial z} = 0 \tag{11}$$

the resulting axial velocity distribution may be found by adding the two radial velocity fields together. It then follows that

$$\left.\begin{aligned} V_z - V_{z,-\infty} &= -\left(\frac{1}{kr}\right)\frac{d}{dr}\left(\frac{rf - rS_r}{2k}\right) e^{kz}, \qquad z<0 \\ V_{z,+\infty} - V_z &= -\left(\frac{1}{kr}\right)\frac{d}{dr}\left(\frac{rf - rS_r}{2k}\right) e^{-kz}, \qquad z>0 \end{aligned}\right\} \tag{12}$$

At the leading and trailing edges of the source/vortex disc the axial velocities are

$$\left.\begin{aligned} V_{z,-0} &= V'_z = V_{z,0} - \frac{S}{2} \\ V_{z,+0} &= V''_z = V_{z,0} + \frac{S}{2} \end{aligned}\right\} \tag{13}$$

where $V_{z,0}$ is the axial velocity exactly in the plane of the disc. From eqs. (12) it may be shown, by subtraction, that

$$\frac{dV_{z,0}}{dr} = \frac{1}{2}\frac{dV_{z,+\infty}}{dr} \tag{14}$$

putting z equal to zero in each equation.

The quantity on the right of eq. (14) is, in fact, half the value of the tangential vorticity on the downstream side of the row and may be found from the equation of radial equilibrium applied at downstream infinity, provided the usual linearization assumptions are made, namely, that at radius r,

$$H(+\infty) = H(-\infty) + \Omega r(V''_\theta - V'_\theta)$$
$$V_\theta(+\infty) = V''_\theta$$

which gives the total energy in terms of the blade work. Eliminating V_θ in terms of relative outlet angle at the disc (which it will be remembered is the usual 'attached flow' value β_2) then the resulting equation for V'_z, the axial velocity in front of the disc, is as follows:

$$\begin{aligned} (2V'_z + 2S + (V'_z + S)t_2^2)\frac{dV'_z}{dr} &= 2\Omega^2 r - \Omega r t'_2 V'_z - \Omega r t'_2 S - \Omega t_2 r S_r - t_2 \Omega V'_z \\ &\quad - t_2 \Omega S - V'_z S_r - S S_r + (V'_z t_2 + S t_2 - \Omega r) \\ &\quad \times \frac{(2\Omega r - V'_z t'_2 r - S t'_2 r - t_2 r S_r - V'_z t_2 - S t_2)}{r} \end{aligned} \tag{15}$$

in which t_2, t'_2 are short for $\tan \beta_2$ and its radial gradient. In this equation use has been made of the first of eqs (13) to eliminate $V_{z,0}$. It is possible to combine eqs (5) and (6) to give

$$\alpha = \frac{\cos \beta_1}{D \cos \beta_2} \tag{15a}$$

which, together with eqs (4) and (5) may be used to obtain S in terms of V'_z, D and β_2; the resulting expression is given in Appendix 1. It is then necessary to obtain S_r in terms of V'_z and its gradient, involving also the inlet angle β_1. These details are also given in Appendix 1,

where the final equation, being rather lengthy, is given in full. It is of the form

$$A \frac{dV'_z}{dr} = B \tag{16}$$

The numerical solution of equations of this type may be obtained using the Runge-Kutta technique once an initial value (at the hub or tip) of the axial velocity V'_z is assumed. In this way, a series of solutions may be constructed corresponding to a range of mass flows. However, an important limitation arises should there be a zero value for the coefficient A somewhere within the range of radius. There are circumstances in the present problem where this condition arises which have important implications. Before discussing these, it is necessary to go into more detail in regard to the dependence of blockage upon local incidence.

A UNIVERSAL BLOCKAGE EQUATION

As pointed out above, the loss process has been divided into a loss-free separation at the blade row exit and a downstream mixing process which latter is being regarded as being unimportant for the flow equilibrium. This model is an oversimplification in view of the fact that a more severe separation might occur at hub and tip (due to three-dimensional effects) while elsewhere, the flow, being nearly two-dimensional, will display a lesser degree of separation. Nevertheless, a blockage value α will be assumed to be, at each radius, a function of inlet angle β_1 alone, but subject to other parameters which would vary with the section (and, therefore, be functions of radius).

It is readily seen, by combining eqs (5) and (6), that the diffusion ratio is given by

$$D = \frac{\cos \beta_1}{\alpha \cos \beta_2} \tag{17}$$

The value of α [given by eq. (1)] may be determined from cascade or rotor tests. It may be seen in Fig. 7 that the condition given by eq. (2), actually in the form of eq. (3), can be attained just prior to stalling. If, in place of these, eq. (17) for D is evaluated and also plotted against cot β_1, it may be shown (see below) that the condition expressed by eq. (2) can only occur when the derivative, $dD/d \cot \beta_1$, is negative, i.e., after it has passed through a minimum. Figure 3 shows the trend which D follows, using experimental data from the rotor mentioned above corresponding to a section 25 mm inward from the tip. It was decided to choose D as a suitable description of a cascade, or blade section, performance because of the following factors: (i) it is well known that the practical (lower) limit to D in a compressor cascade is around 0·7 (this value being equivalent to a de Haller number of 0·51); (ii) that the curve must approach (more-or-less closely) around design incidences, the curve for loss-free flow, which corresponds to α equal to unity, namely, $D = \cos \beta_1 / \cos \beta_2$; and (iii) the degree of blockage occurring at the minimum diffusion, α_m, locates the position of the minimum along the abscissa. In fact, it is convenient to change the abscissa from cot β_1 to the ratio Y given by

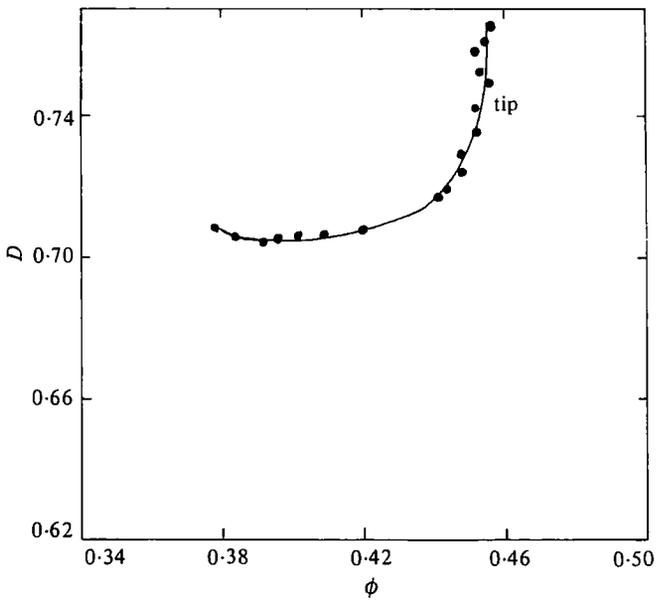

Fig. 3. The variation of the diffusion factor with the local flow coefficient for a section close to tip

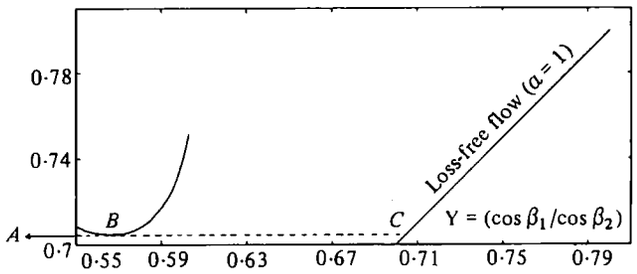

Fig. 4. The variation of the diffusion factor with Y for the section close to tip

$$Y = \frac{\cos \beta_1}{\cos \beta_2}$$

for then the line $Y = D$ represents loss-free flow and the ratio, AB/AC in Fig. 4, is the value of α_m at D equal to D_M. It is thus possible to write the D-function in the form

$$D = D(Y, \alpha_m, D_m) \tag{18}$$

where D_m the minimum diffusion ratio; evaluated via eqs. (1) and (5a) (corresponding with near maximum pressure rise) and α_m, the blockage at minimum diffusion ratio, may each be determined from experimental data. The form of the above function is then easily constructed since it has concave-upward form at the minimum ratio. In the analysis, the derivative of D with respect to radius will be required, hence a simple analytic form is essential in order that this derivative may be obtained as follows:

$$\frac{dD}{dr} = \frac{\partial D}{\partial Y}\frac{dY}{dr} + \frac{\partial D}{\partial \alpha_m} \cdot \frac{d\alpha_m}{dr} + \frac{\partial D}{\partial D_m} \cdot \frac{dD_m}{dr} \tag{19}$$

In the results presented herein, a variation of α_m and D_M upon radius has been allowed but in evaluating the gradient of D, the second and third terms in eq. (19) were ignored. This permitted the use of a more complex relationship; in fact a fourth-degree polynomial in terms of the quantity, $(\cot \beta_1 - \cot \beta_{1,0})$, where the suffix '0' denoted the point at which the loss starts to increase from zero was assumed. However, this curve does not attempt to achieve correct loss values at lower incidences.

DISCUSSION OF EQUATION FOR AXIAL VELOCITY

Having determined the analytical form of D, the coefficient, A, in eq. (16) may be examined. Referring to Appendix 1 it will be seen that the coefficient may be expressed in terms of the function, $C(r)$ there used. Equating this to zero determines the circumstance in which a singularity appears in the solution for V_z'. This condition is

$$(1 + \sec^2 \beta_2 \,.\, C(r))(V_z' + S) = 0 \qquad (20)$$

The condition $V_z' = -S$ represents an extreme case, therefore, the condition under which the first bracket becomes zero is examined. Substituting for $C(r)$ from the Appendix it is evident that the condition for a singular solution is given by:

$$\frac{dD}{d(\cot \beta_1)} = D_s' = -\cos \beta_2 \left(\frac{D \sin 2\beta_1}{2 + \sin \beta_1}\right) \qquad (21)$$

and it should be noted that the source intensity (other than through its relationship to D) does not occur. A proper analytical treatment of the singularity need not be carried out, since the real flow would break down into another regime before infinite gradients could be approached. In addition the linearization assumptions inherent in the treatment would begin to be violated. Further examination of eq. (21) reveals that the above condition is reached after the condition for the instability to small disturbances, namely, that given by eq. (2). It may be shown, using eq. (2) that this latter condition is also given by

$$\frac{dD}{d(\cot \beta_1)} = -\tfrac{1}{2} D \sin 2\beta_1 \qquad (22)$$

Dividing eq. (21) by eq. (22) it may also be shown that the ratio of slopes is given by

$$\cos \beta_2 + \frac{1}{\alpha D^2}$$

Since both α and D are less than unity, it is thus seen that small disturbance instability must precede the appearance of the singularity limit.

NUMERICAL SOLUTION

The numerical solution of eq. (16) (full equation given in Appendix 1) may be proceeded with once the presence of the singularity is known. For reasons connected with the form of the solution it has been found that integration

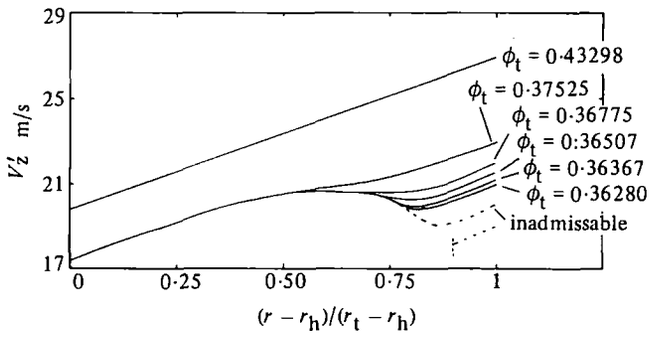

Fig. 5. Axial velocity variation along span

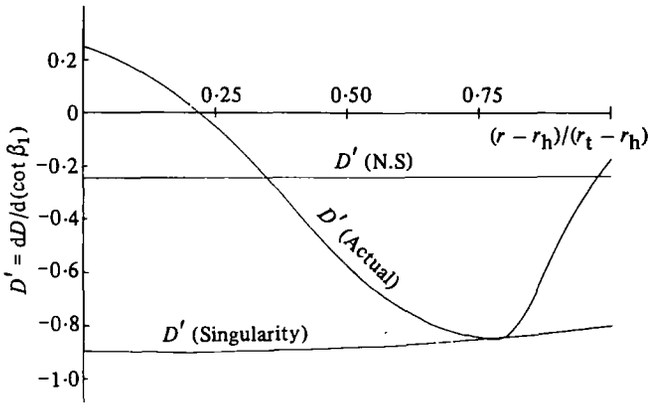

Fig. 6. Variation of D' along span

should commence from the tip, marching inwards towards the hub. For high values of V_z', the solution is obtained with the aid of the appropriate computer library routines and an example is shown in Fig. 5 for $V_z'(r_t)$ at the tip, of 27 m/s. The mass flow is found after the solution and is expressed in terms of ϕ_t given by $V_z'/\Omega r_t$. As $V_z'(r_t)$ is reduced, the solution takes on a limiting form over, in this example, the inner 65 per cent of blade height. Thus change in V_z' with reducing mass flow is confined to the outer 35 per cent until a point is reached when the integration process breaks down (because the range now contains a singularity). The numerical routine now, properly, 'fails' indicating also a physical limitation inasmuch as an infinite gradient is not meaningful. The dotted line shown corresponding to a $V_z'(r_t)$ of 20 m/s is, in fact, inadmissible since the numerical routine has succeeded in 'jumping' the singularity; therefore, it must be excluded. For $V_z'(r_t)$ equal to 19 m/s, the integration fails at 90 per cent of blade height.

The behaviour of D' over the blade height is shown plotted in Fig. 6 and it is evident that the flow is unstable to small disturbances between 35 and 97 per cent of blade height. It is also clear that the above limiting V_z' solution just reaches the singularity limit at 77·5 per cent of height. It is possible to calculate from the range of solutions the local $\psi_2 - \phi$ characteristics for three blade sections at radii of 0·5009 m (25 mm from the hub), 0·4387 m at mid-blade-height, and 0·3764 m (25 mm from the tip). These are shown plotted in Fig. 7, and also given, are experimental curves for a single rotor having the same dimensions and a relative outlet angle variation close to the variation assumed for the above calculation (see Appendix 2). The variation of D_M and α_m used in the above calculation was obtained from experiment, although it should be noted that the minimum diffusion factor point was only passed near the tip and hub of the experimental rotor. Nevertheless, the values of D_M and α_m used were taken from the experimental results at points as close as possible to the minimum D; these values are also given in Appendix 2.

The question naturally arises as to the existence of solutions corresponding to values of V_z' which are everywhere sufficiently low so as not to contain the singularity within the range of radius. These results will lie on the D–Y curve to the left of the critical value (see Fig. 4) and will give rise to meaningful solutions. However, the resulting integrated pressure-volume characteristic (an

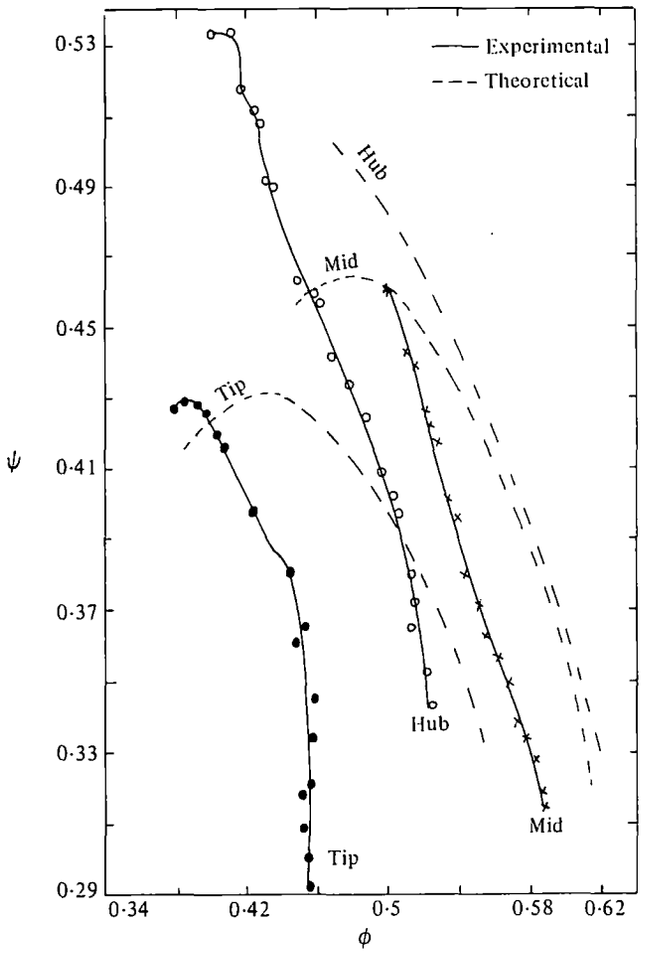

Fig. 7. Transverse results (total-to-state pressure coefficients)

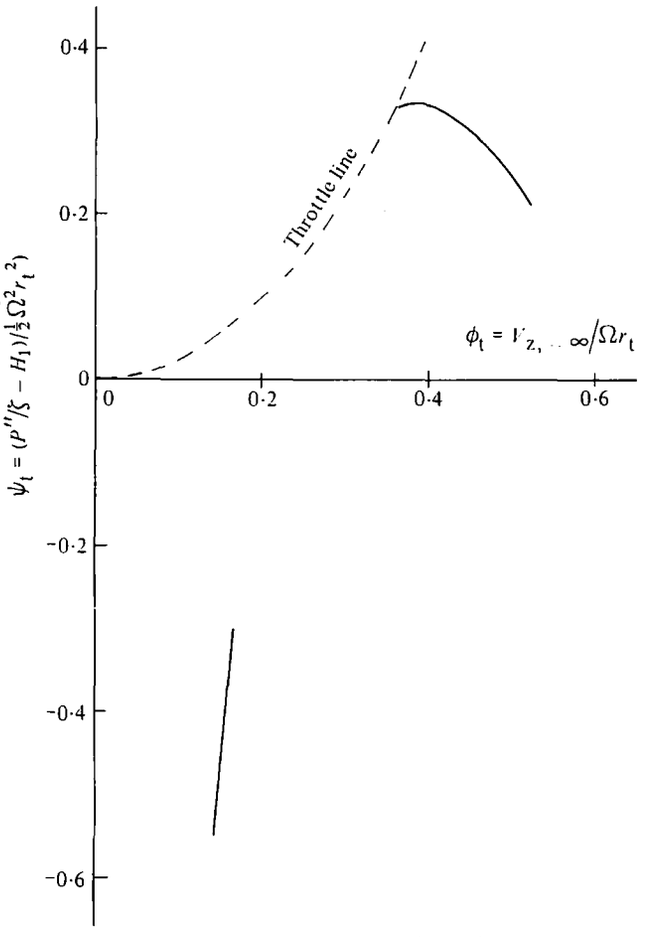

Fig. 8. The integrated pressure volume characteristic

example is shown in Fig. 8) will exhibit a 'gap' which indicates that this portion of the characteristic is not accessible by throttle valve adjustment (a fixed setting of which will allow a roughly parabolic dependence of pressure on volume). In any case, every point across the radius for these 'beyond critical' points is unstable to small disturbances, i.e., the slopes are more negative than is given by eq. (22).

A further question arises: what might be the effect on the above performance if each blade section were to reach its minimum diffusion ratio at a smaller or larger value of blockage (i.e., what would be the effect on a series of rotors of differing α_m)? Some indication of this is given in Fig. 9 where the limit of stable (to small disturbance) operation $\phi_{t,n}$ and the 'singularity' limit $\phi_{t,c}$ is plotted against α_m. In this example values of α_m lower than 0·725 allow the axial velocity to reach zero before the limit is reached. The implication here is that a regime of 'reverse flow', near the hub in this example, will intervene.

GENERAL DEDUCTIONS FROM THE MODEL

The conclusion is drawn that the theoretical model of the blade row presented above predicts a unique breakdown of the normal flow regime by a mechanism unrelated to that of small disturbance instability. The breakdown is preceded by the appearance of a limiting distribution (over part of the radius), followed by the appearance of a 'hole' in the axial velocity distribution

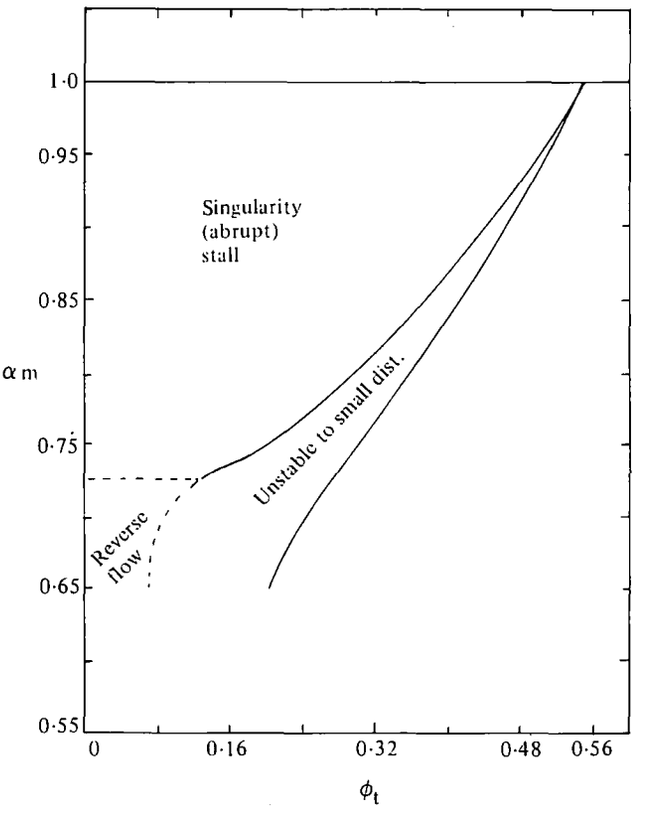

Fig. 9. Theoretical map of performance: tan $\beta_2 = 0{\cdot}8391$ and $D_m = 0{\cdot}7$

which is physically to be regarded as a breakdown. The fact that the real blade row passes irreversibly into a deep stall regime is an indication that a different, alternative, regime has been found. Reasonable agreement between experimental and predicted characteristics is demonstrated. However, it should be noted that the D-curves used in the numerical predictions passed much more closely to the loss-free D-curve than did the experimental curves. Had D-curves been used which resembled the experimental ones in the lower incidence region, results much closer to the experimental pressure rise characteristics would have been obtained. However, it is more important here to concentrate upon flow coefficients in the neighbourhood of the theoretical limit.

The realization that there are abrupt limitations to the behaviour of axial compressor rows had been appreciated firstly by McKenzie (3) who developed a theory, using simple radial equilibrium at row exit, which was able to predict the shape of the pressure-volume characteristic up to stall. Secondly, Fabri (4), also assuming simple radial equilibrium at rotor exit, demonstrated that by using the earlier hydraulic 'shock-loss' model, then a condition could arise in which the controlling equation became singular. He attributed the appearance of rotating stall to the presence of this condition.

The analysis presented above has the virtue of simplicity but at the same time represents a linearization of the equations of motion. It would seem a worthwhile objective to carry out a completely non-linear analysis of the same problem to gain more physical insight to the model.

ACKNOWLEDGEMENTS

The authors wish to acknowledge the support of the Science Research Council and Rolls-Royce Limited for their support. They also wish to thank C. Freeman and A. B. McKenzie of Rolls-Royce for valuable discussions.

REFERENCES

(1) STENNING, A. H., and KRIEBEL, A. R. 'Stall Propagation in a Cascade of Airfoils', *Trans. ASME*, May 1958

(2) MARBLE, F. E. 'The Flow of a Perfect Fluid through an Axial Turbo-Machine with Predescribed Blade Loading', *J. Aero. Sci.*, Aug. 1948

(3) MCKENZIE, A. B. (Rolls-Royce internal report), 1962

(4) FABRI, J. 'Rotating Stall in an Axial-flow Compressor' *Internal Aerodynamics* (*IMechE*, 1970), 96–110

(5) AL-DAINI, A. J., and RAILLY, J. W. 'A Theoretical Criterion for Abrupt Stall in Axial Flow Compressors', Department of Mechanical Engineering, Birmingham University, Research Report No. 161, Mar. 1978

(6) AL-DAINI, A. J. 'An Investigation of the Stability of Isolated Axial Compressor Rows', *Ph.D. Thesis*, Birmingham University, 1979

APPENDIX 1

Evaluation of S and S_r in terms of V'_z, D and β_2.
From eqs. (4), (5), and (5a) namely:

$$S = V''_z - V'_z \tag{1.1}$$

$$\alpha = V'_z/V''_z \tag{1.2}$$

and

$$\alpha = \cos\beta_1/D\cos\beta_2 \tag{1.3}$$

Substituting for V''_z from (1.1) into (1.2) and putting $\cos\beta_1 = V'_z/(V'^2_z + \Omega^2r^2)^{1/2}$ into eq. (1.3), and equating the two resulting equations gives

$$S = D(V'^2_z + \Omega^2r^2)^{1/2}\cos\beta_2 - V'_z \tag{1.4}$$

putting $Q^2 = V'^2_z + \Omega^2r^2$ the above equation becomes

$$S = DQ\cos\beta_2 - V'_z$$

differentiating the above equation with respect to r gives

$$S_r = -DQ\sin\beta_2\frac{d\beta_2}{dr} + \left(\frac{D\cos\beta_2}{Q}\right)\left|V'_z\frac{dV'_z}{dr} + \Omega^2r\right| + Q\cos\beta_2\frac{dD}{dr} - \frac{dV'_z}{dr} \tag{1.5}$$

In evaluating dD/dr, only the first term of eq. (19) is used, thus

$$\frac{dD}{dr} = \frac{dD}{d(\cot\beta_1)}\cdot\frac{d(\cot\beta_1)}{dr} \tag{1.6}$$

Now

$$\cot\beta_1 = \frac{V'_z}{\Omega r}$$

differentiating the above with respect to r and substituting in eq. (1.6) gives

$$\frac{dD}{dr} = \frac{D'}{\Omega r}\left|\frac{dV'_z}{dr} - \frac{V'_z}{r}\right| \tag{1.7}$$

where

$$D' = \frac{dD}{d(\cot\beta_1)}$$

Substituting eq. (1.7) in (1.5) gives

$$S_r = -DQ\sin\beta_2\frac{d\beta_2}{dr} + \frac{D\cos\beta_2}{Q}\left|V'_z\frac{dV'_z}{dr} + \Omega^2r\right| + \frac{Q\cos\beta_2 D'}{\Omega r}\left(\frac{dV'_z}{dr} - \frac{V'_z}{r}\right) - \frac{dV'_z}{dr}$$

Substituting for S_r in equation 15 gives the final equation of the system as

$$\begin{aligned}(V'_z + S)(1 + \sec^2\beta_2 \,.\, C(r))\frac{dV'_z}{dr} &= 2\Omega^2r - \Omega rt'_2V'_z - \Omega rt'_2S - t_2\Omega V'_z - t_2\Omega S \\ &\quad + (V'_z + St - \Omega r) \\ &\quad \times \frac{2\Omega r - V'_zt'_2r - St'_2r - V'_zt_2 - St_2}{r} \\ &\quad + E(r)\,.\,(V'_z + S + V'_zt_2^2 + St_2^2)\end{aligned} \tag{1.8}$$

where

$$C(r) = \frac{DV'_z\cos\beta_2}{Q} + \frac{Q\cos\beta_2 D'}{\Omega r}$$

$$E(r) = \frac{D\Omega^2r\cos\beta_2}{Q} - DQ\sin\beta_2\frac{d\beta_2}{dr} - \frac{QV'_zD'\cos\beta_2}{\Omega r^2}$$

APPENDIX 2

Details of Rotor Tested

The rotor tested has a C_4 base profile, 9 per cent maximum thickness (30 per cent from L.E.), circular arc camber (number of blades = 20).

Blade section	Camber (degrees)	Stagger (degrees)	Chord length (mm)	α_m	D_m	β_2°
Root	45·00	44·5	152	0·75	0·631	39
Mean	45·00	49·6	152	0·9	0·657	40
Tip	45·00	54·7	152	0·8	0·705	47